J. prakt. Chem. 339 (1997) 708–713

Journal für praktische Chemie
Chemiker-Zeitung

Tetrahedral Adamantane Derivatives: Glass Formation and Melting Behaviour

D. Braun and C.-C. Keller

Darmstadt, Deutsches Kunststoff-Institut

M. D. Roth, B. Schartel, M. Voigt and J. H. Wendorff

Marburg, Fachbereich Chemie, Institut für Physikalische Chemie, Kernchemie und Makromolekulare Chemie und Wissenschaftliches Zentrum für Materialwissenschaften, Philipps-Universität

Received July 23rd, 1997 respectively September 22nd, 1997

Abstract. The influence of the chemical structure of rigid star-shaped multipodes composed of an adamantane central core and short rigid branches on the glass formation and crystallisation is analysed. It was found that esters of 1,3,5,7-adamantanetetracarboxylic acid with various phenols (**3a–c**) and esters of 1,3,5,7-tetrahydroxyadamantane with various benzoic acid derivatives (**4a–c**) display both crystalline and glassy states with high glass transition temperatures and melting temperatures. These quantities strongly depend on the restriction of the rotational motions about the ester groups connecting the core and the branches.

It is a general observation that the shape of organic molecules contributes significantly to the thermodynamic, structural and dynamic properties of the condensed state. Plastic crystals displayed by spherical molecules and liquid crystalline phases displayed by rod-like or disc-shaped molecules are examples in case [1, 2]. Based on lattice calculations we were able to show that rigid multipodes, *i.e.* rigid cross-shaped or star-shaped molecules, should be characterized by a strongly enhanced thermodynamic compatibility with organic low molar mass and polymer compounds [3–5]. In addition, we expect that such molecules should have a reduced tendency towards crystallisation and – since their motion in the condensed state requires large amounts of free volume – should be distinguished by high glass transition temperatures. Organic low molar mass materials displaying high glass transition temperatures of the order of 100 °C and above meet with considerable interest with respect to applications involving guest–host systems [5, 6]. Examples in case are Non-Linear-Optical (NLO) active systems for second harmonic generation (SHG) or for electro–optical modulations (Pockels-effect) [6]. The matrix is currently composed in the majority of cases of polymers which provide good film forming capabilities and mechanical properties. Yet, polymer-based guest–host systems have some serious disadvantages: the miscibility of the chromophores is often limited to a few percent for entropic reasons. One is therefore interested in low molar mass compounds displaying high glass transition temperatures.

We consider in this contribution star-shaped molecules based on a central adamantane core and we correlate chemical modifications with the corresponding variations of the thermodynamic and structural properties. The influence of the linkage between the core and the branches is of particular interest.

Results and Discussion

To investigate the influence of the linkage, several derivatives of 1,3,5,7-adamantanetetracarboxylic acid and 1,3,5,7-tetrahydroxyadamantane were synthesised and the glass-forming properties of these constitutional isomers were studied. The derivatives of the 1,3,5,7-adamantanetetracarboxylic acid were obtained by esterification of the phenol compounds with 1,3,5,7-adamantanetetracarboxylic acid chloride **1** in pyridine.

The esterification of 1,3,5,7-tetrahydroxyadamantane **2** with the corresponding benzoyl chlorides under the same conditions leads to the constitutional isomers.

This variation of the linkage will strongly influence the rotational motions about the bonds connecting the core and the branches. The carbonyl oxygens face the space-filling adamantane core in the compounds **4a–c** while the CO groups face the less space-filling phenyl groups in the compounds **3a–c**. Fig. 1 displays the two-

dimensional rotational potentials for the two cases.

The finding is that the rotation about the Ad-CO bond

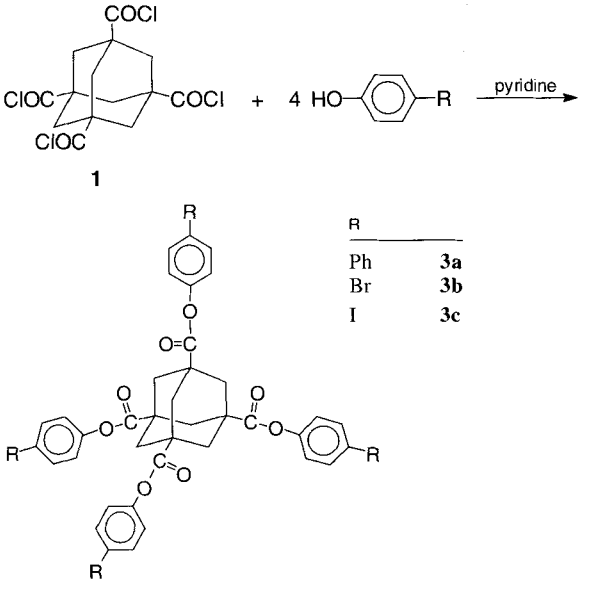

Scheme 1 Preparation of the adamantane derivatives **3**

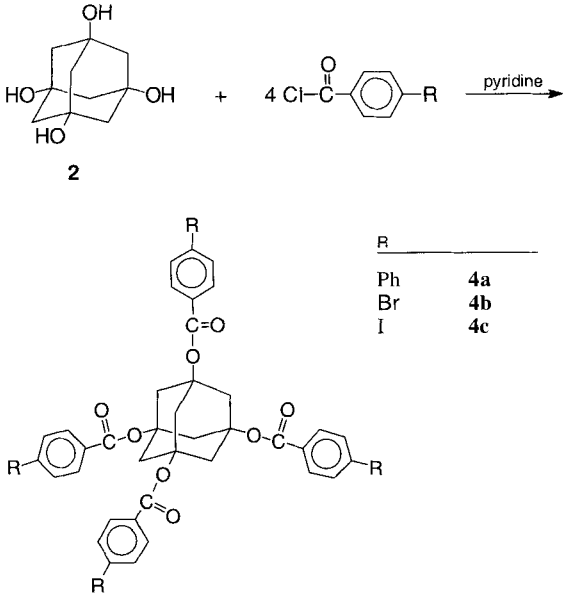

Scheme 2 Preparation of the adamantane derivatives **4**

at fixed rotational angle of the CO–O bond is constrained by rotational barriers with a barrier height of approximately 12 kJ/mol (compounds **3**) whereas the rotational potential of the Ad-O-bond (at fixed rotational angle of the O–CO bond) displays several rotational

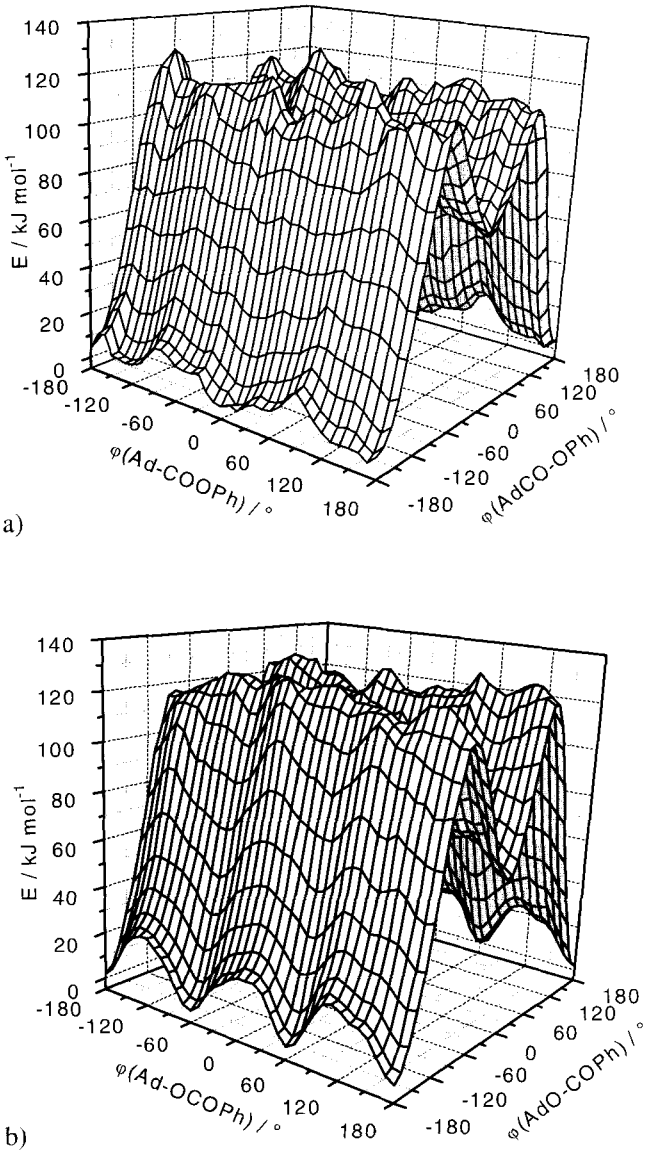

Fig. 1 Two-dimensional rotational potentials of the esters of 1,3,5,7-adamantanetetracarboxylic acid (**3**) (a) and the esters of 1,3,5,7-tetrahydroxyadamantane (**4**) (b) as obtained from force field calculations

barriers with a barrier height of approximately 24 kJ/mol in the case of the compounds **4**.

In order to get a more detailed insight into the local chain dynamics of the internal bonds considered here we studied the evolution of torsional angles versus time for 300 K. The resulting distributions of torsional angles are displayed in Fig. 2. It is apparent that the preferred conformation of the fragment $(H_2C)_3$–C–O–CO in the compounds **4** is a staggered conformation (φ(Ad-OCOPh) = ± 60°, ± 180°). In the compounds **3** the fragment $(H_2C)_3$–C–CO–OPh prefers an ecliptic conformation (φ(Ad-COOPh) = 0°, ± 120°), but also the staggered conformation is populated to a considerable

amount. This indicates again the differences in internal mobility of the two types of compounds.

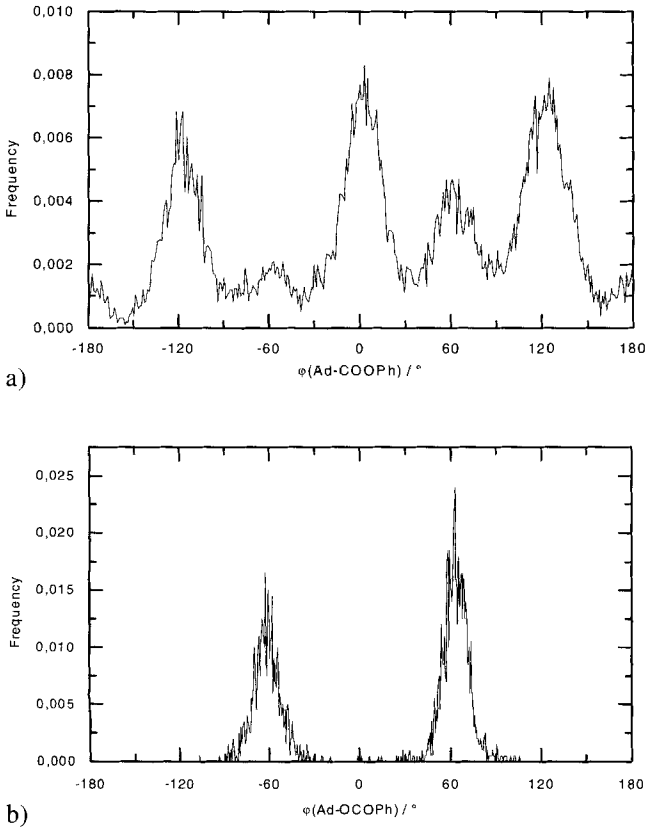

Fig. 2 Distribution of torsional angles at a temperature of 300 K as obtained from molecular dynamics calculations, a) esters of 1,3,5,7-adamantanetetracarboxylic acid (**3**), b) esters of 1,3,5,7-tetrahydroxyadamantane; simulation time limited to 100 ps (**4**)

Thus, the expectation is that the constrained rotational motion of the compounds **4** will affect not only dynamic but also structural and thermodynamic properties. The experimental finding is that all compounds are able to crystallise, yet can also be transferred into the glassy state. Fig. 3 displays the X-ray scattering data obtained for the glassy state of compound **4a**. It is characterised by a broad asymmetric halo which results from the superposition of two halos. Similar diagrams were obtained for an adamantane derivative where the biphenyl unit was coupled directly to the adamantane core [7]. The X-ray diagrams of the crystalline samples display a large number of narrow Bragg peaks. However, the poor quality of the crystals did not allow the determination of the crystal structure.

Tab. 1 displays both the glass transition temperatures and the melting temperatures of the derivatives considered here. We will concentrate, at first, on the location

Tab. 1 Glass and melting temperatures of the adamantane derivatives **3** and **4**

Compound	T_m/°C	T_g/°C
3a	166 (180 [a])	87
4a	267	116
3b	225	64 [b]
4b	243 (257 [a])	102 [b]
3c	277	75 [b]
4c	295	118

[a]) Obtained in first heating run.
[b]) Obtained after quenching in liquid N_2.

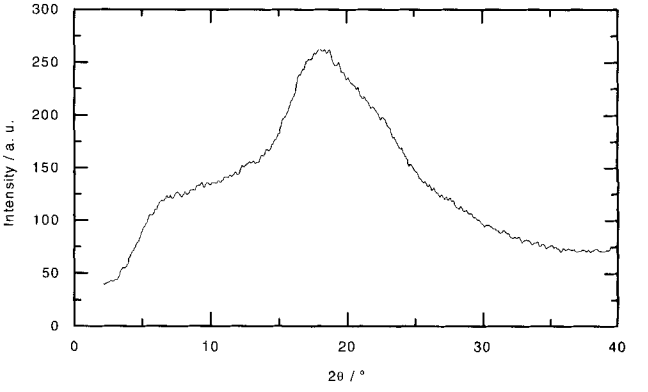

Fig. 3 Scattering diagram of 1,3,5,7-tetrakis([1,1'-biphenyl]-4-carbonyloxy)adamantane (**4a**) in the amorphous state

of the glass transition temperatures. It is apparent from Tab. 1 that the glass transition temperatures of the compounds derived from **2** are 30 to 40 °C higher than those of the corresponding compounds derived from **1**. Characteristic examples are the compounds **3c** and **4c** for which we observe a difference of about 40 °C. This shift is independent of the substituents R while the absolute values of the glass transition temperatures depend on the nature of the substituent. It is apparent that these adamantane derivatives are interesting glass-forming materials. It is instructive to compare the results reported with those obtained for other derivatives. In fact, several papers were concerned with similar compounds [7–10]. The direct coupling of the biphenyl unit to the adamantane core leads to a glass transition temperature which is reported to be as high as 151 °C [11]. The absolute value seems to depend quite strongly on the degree of purity.

An inspection of Tab. 1 leads to the conclusion that it is not only the glass transition temperature which is affected by the rotational degrees of freedom but also the melting behaviour. The compounds displaying lower glass transition temperatures also display lower melting temperatures. The shifts vary between 20 and 100 °C. A closer inspection of the crystallisation data

is, however, needed since the solid states may differ significantly. We will discuss only results obtained for samples which have been melted at least once prior to the thermal analysis in order to reduce effects of the thermal history.

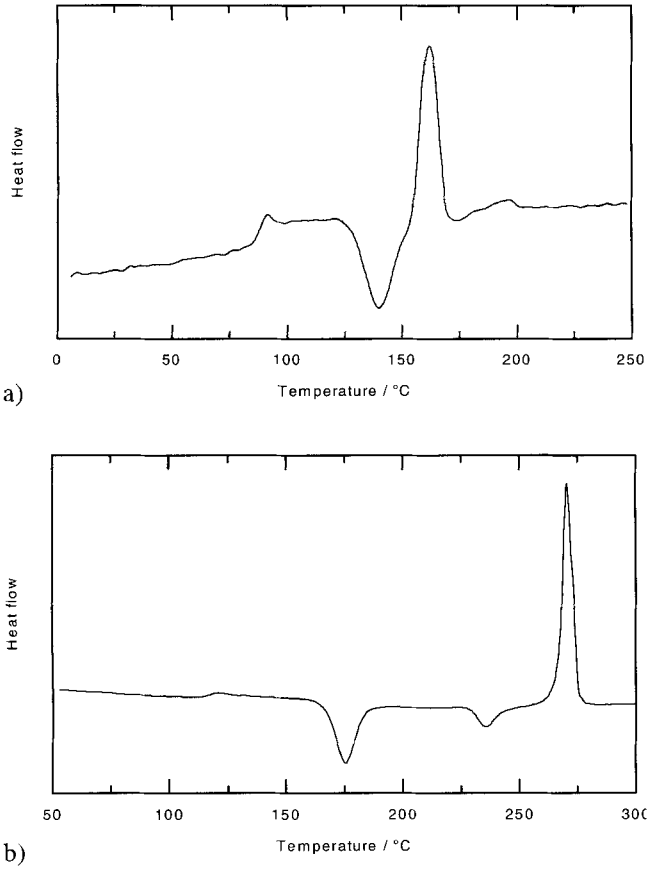

Fig. 4 DSC-diagrams of 1,3,5,7-adamantanetetracarboxylic acid tetrakis([1,1'-biphenyl]-4-yl) ester (**3a**) (a) and 1,3,5,7-tetrakis([1,1'-biphenyl]-4-carbonyloxy)adamantane (**4a**) (b)

Compound **3a** displays a single melting temperature amounting to 166 °C (Fig. 4a). The constitutional isomer **4a**, on the other hand, is characterised by a melting temperature which is approximately 100 K above the one of the compound **3a**, it melts at 267 °C (Fig. 4b). The direct coupling of the biphenyl unit to the adamantane core leads to a much higher melting temperature which was reported to be as high as 408 °C [11]. Both samples obviously are only partially crystalline after cooling from the melt. The DSC diagram reveals a glass transition temperature and one exothermic peak for compound **3a** prior to the melting peak. The exothermic peak indicates the onset of a crystallisation process during the heating cycle. The compound **4a** displays an even more complex behaviour: it shows two exothermic peaks. A further observation is that morphological changes take place in the temperature range where the second exothermic peak is observed: spherulites are transformed into needle-shaped crystalline regions. This is shown in Fig. 5.

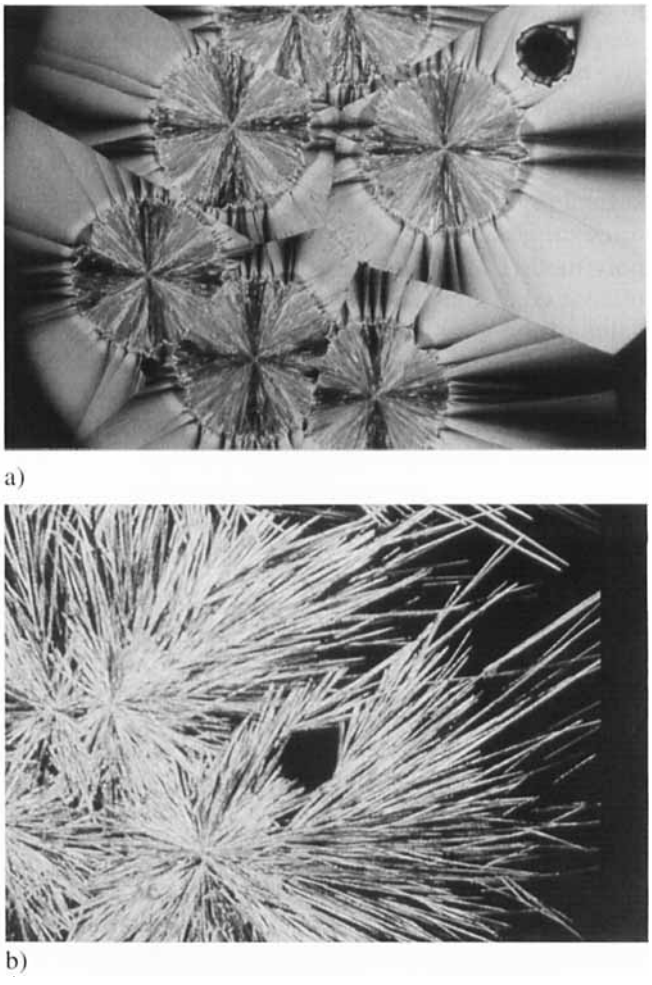

Fig. 5 Morphology of 1,3,5,7-tetrakis([1,1'-biphenyl]-4-carbonyloxy)adamantane (**4a**) below (a) and above (b) a temperature interval of 240–245 °C, respectively

It is thus obvious that the structure formation is controlled by kinetic hindrances in the case of compound **4a** and less so in the case of compound **3a**. This difference in the character of the crystallisation and melting behaviour is observed for all compounds. Compound **3b** showed in DSC measurements two endothermic transitions at 218 and 225 °C, which were observed also in further heating runs. We attribute them to different crystal modifications. Compound **4b** showed a melting transition at 243 °C. Compound **3c** displays only one endothermic transition at 277 °C and compound **4c** a melting temperature of 295 °C. Exothermic transitions are observed again in the heating runs for the compounds **4b** and **4c**.

It thus seems that the crystallisation behaviour differs significantly for the series **3** and **4** considered here.

The nature of the groups R affects the absolute values of the melting temperatures but not the character of the crystallisation and melting behaviour. Finally, we have to point out that NMR results revealed the presence of water in all compounds synthesised, in spite of intensive drying. No fixed molar ratio of the mixture water/compound could be found; further investigations on this subject are necessary.

The general conclusions are that small rigid star-shaped organic molecules may display glass temperatures surpassing those of amorphous polymers such as poly(methyl methacrylate) or polystyrene, which are often used in guest–host systems, and that the absolute value of the glass transition temperature may be controlled by internal degrees of rotational freedom.

We gratefully acknowledge the financial support by the Deutsche Forschungsgemeinschaft (DFG).

Experimental

Pyridine, 4-hydroxybiphenyl, 4-bromophenol, 4-iodophenol, [1,1'-biphenyl]-4-carbonyl chloride, 4-bromobenzoyl chloride (Acros) and 4-iodobenzoyl chloride (Aldrich) were used as received. Silica gel for chromatography was Merck silica gel 60 (0.063–0.200 mm). DSC measurements were performed on a DuPont 912 Dual Sample Differential Scanning Calorimeter and a Mettler Differential Scanning Calorimeter type DSC 30 at a heating rate of 10 K min^{-1}. ^1H NMR spectra were recorded on a Bruker WM 300 spectrometer. Microscopy investigations were performed with a Laborlux 12 ME ST microscope (Leitz), using a THMS600 heating freezing stage connected to a TP 91 controller (Linkam). The X-ray diagrams were obtained using a D500 diffractometer (Siemens). The rotational potentials were calculated on the basis of a force field approach. The program Cerius^2 of Molecular Simulations Inc. [12] was chosen to carry out these calculations and we used the DREIDING force field by Goddard III *et al.* [13].

1,3,5,7-Adamantanetetracarboxylic acid was obtained according to the method of Newkome *et al.* [14]. 1,3,5,7-Tetrahydroxyadamantane **2** was prepared as described by Stetter and Krause [15].

1,3,5,7-Adamantanetetracarboxylic Acid Chloride (1)

A mixture of 4.5 g (14 mmol) 1,3,5,7-adamantanetetracarboxylic acid and 20 ml $SOCl_2$ was refluxed for 4 h, excess $SOCl_2$ was removed *in vacuo*. The crude product was purified by sublimation, resulting in 3.4 g (61%) of a white powder, *m. p.* 145 °C (further phase transitions were observed at 115 and 143 °C).

Synthesis of Esters of 1,3,5,7-Adamantanetetracarboxylic Acid (3a–c) (General Procedure)

Acid chloride **1** (1 equiv.) and the phenolic component (5 equiv.) were dissolved in 40 ml pyridine and stirred at 80 °C for 16 h. The solution was poured into a mixture of ice and 1M HCl, the precipitate was filtered, dissolved in $CHCl_3$, precipitated in methanol, filtered again and purified by chromatography eluting with $CHCl_3$.

1,3,5,7-Adamantanetetracarboxylic acid tetrakis([1,1'-biphenyl]-4-yl) ester (**3a**)

was obtained from **1** and 4-hydroxybiphenyl; yield 69%, *m. p.* 166 °C (further heating runs). – ^1H NMR ($CDCl_3$): δ/ppm = 2.52 (s, 12 H); 7.22 (d, 8 H), 7.38 (t, 4 H), 7.44 (t, 8 H), 7.58 (d, 8 H), 7.63 (d, 8 H).

1,3,5,7-Adamantanetetracarboxylic acid tetrakis(4-bromophenyl)ester (**3b**)

was obtained from **1** and 4-bromophenol; yield 65%, *m. p.* 225 °C (further phase transition at 218 °C). – ^1H NMR ($CDCl_3$): δ/ppm = 2.41 (s, 12 H), 7.00 (d, 8 H), 7.52 (d, 8 H).

1,3,5,7-Adamantanetetracarboxylic acid tetrakis(4-iodophenyl)ester (**3c**)

was obtained from **1** and 4-iodophenol; yield 63%, *m. p.* 277 °C. – ^1H NMR (THF-d_8): δ/ppm 2.41 (s, 12 H), 6.97 (d, 8 H), 7.73 (d, 8 H).

Synthesis of Esters of 1,3,5,7-Tetrahydroxyadamantane (4a–c) (General Procedure)

1,3,5,7-Tetrahydroxyadamantane **2** (1 equiv.) and the benzoyl chloride component (5 equiv.) were dissolved in 40 ml pyridine and stirred at 80 °C for 16 h. The further procedure was as described above.

1,3,5,7-Tetrakis([1,1'-biphenyl]-4-carbonyloxy)adamantane (**4a**)

was obtained from **2** and [1,1'-biphenyl]-4-carbonyl chloride; yield 67%, *m. p.* 267 °C (an exothermic phase transition is observed between 220 and 250 °C). – ^1H NMR ($CDCl_3$): δ/ppm = 3.02 (s, 12 H), 7.40 (t, 4 H), 7.48 (t, 8 H); 7.65 (overlap d, d, 16 H); 8.08 (d, 8 H).

1,3,5,7-Tetrakis(4-bromobenzoyloxy)adamantane (**4b**)

was obtained from **2** and 4-bromobenzoyl chloride; yield 61%, *m. p.* 257 °C (first heating), 243 °C (further heating runs). – ^1H NMR (THF-d_8): δ/ppm = 2.93 (s, 12 H), 7.65 (d, 8 H), 7.92 (d, 8 H).

1,3,5,7-Tetrakis(4-iodobenzoyloxy)adamantane (**4c**)

was obtained from **2** and 4-iodobenzoyl chloride; yield 62%, *m. p.* 295 °C – ^1H NMR (THF-d_8): δ/ppm = 2.91 (s, 12 H), 7.74 (d, 8 H), 7.85 (d, 8 H).

References

[1] L. A. K. Stavely, Annual Rev. Phys. Chem. **13** (1962) 351

[2] a) P. G. de Gennes, "The Physics of Liquid Crystals", Clarendon, Oxford, Reprint 1975, p. 3; b) S. Chandrasekhar, B. K. Sadashiva, K. A Suresh, Pramãna **9** (1977) 471

[3] U. Gallenkamp, PhD Thesis, Darmstadt 1989

[4] D. Braun, M. Reubold, W. Wegmann, J. H. Wendorff, Makromol. Chem., Rapid Commun. **12** (1991) 151

[5] B. Schartel, V. Stümpflen, J. Wendling, J. H. Wendorff, Polymers for Advanced Technologies **7** (1996) 160
[6] D. J. Williams in "Nonlinear Optical Properties of Organic Molecules and Crystals", D. S. Chemla, J. Zyss, Eds., Academic Press, New York 1987, Vol. 1, p. 405
[7] R. Neuhaus, B. Schartel, V. Stümpflen, J. Wendling, J. H. Wendorff, W. Heitz, Colloid Polym. Sci. **274** (1996) 911
[8] L. J. Mathias, V. R. Reichert, A. V. G. Muir, Chem. Mat. **5** (1993) 4
[9] V. R. Reichert, L. J. Mathias, Polym. Prep. (Am. chem. Soc., Div. Polym. Chem.) **34** (1993) 495
[10] V. R. Reichert, L. J. Mathias, Macromolecules **27** (1994) 7015
[11] V. Stümpflen, Master Thesis, Marburg 1994
[12] Cerius^2, Release 2.0, BIOSYSM/Molecular Simulations, San Diego 1995
[13] S. L. Mayo, B. D. Olafson, W. A. Goddard, J. Chem. Phys. **94** (1990) 8891
[14] G. R. Newkome, A. Nayak, R. K. Behera, C. N. Moorefield, G. R. Baker, J. Org. Chem. **57** (1992) 358
[15] H. Stetter, M. Krause, Liebigs Ann. Chem. **717** (1968) 60

Address for correspondence:
Prof. Dr. Dr. h. c. Dietrich Braun
Deutsches Kunststoff-Institut
Schloßgartenstraße 6
D-64289 Darmstadt